

Spring 5-31-2017

## High performance lattice boltzmann method yield-stress calculations based on intravital images of clot formation in live mice

Vishnu Deep Chandran  
*New Jersey Institute of Technology*

Follow this and additional works at: <https://digitalcommons.njit.edu/theses>



Part of the [Chemical Engineering Commons](#)

---

### Recommended Citation

Chandran, Vishnu Deep, "High performance lattice boltzmann method yield-stress calculations based on intravital images of clot formation in live mice" (2017). *Theses*. 14.  
<https://digitalcommons.njit.edu/theses/14>

This Thesis is brought to you for free and open access by the Electronic Theses and Dissertations at Digital Commons @ NJIT. It has been accepted for inclusion in Theses by an authorized administrator of Digital Commons @ NJIT. For more information, please contact [digitalcommons@njit.edu](mailto:digitalcommons@njit.edu).

## **Copyright Warning & Restrictions**

The copyright law of the United States (Title 17, United States Code) governs the making of photocopies or other reproductions of copyrighted material.

Under certain conditions specified in the law, libraries and archives are authorized to furnish a photocopy or other reproduction. One of these specified conditions is that the photocopy or reproduction is not to be “used for any purpose other than private study, scholarship, or research.” If a user makes a request for, or later uses, a photocopy or reproduction for purposes in excess of “fair use” that user may be liable for copyright infringement,

This institution reserves the right to refuse to accept a copying order if, in its judgment, fulfillment of the order would involve violation of copyright law.

**Please Note: The author retains the copyright while the New Jersey Institute of Technology reserves the right to distribute this thesis or dissertation**

Printing note: If you do not wish to print this page, then select “Pages from: first page # to: last page #” on the print dialog screen

The Van Houten library has removed some of the personal information and all signatures from the approval page and biographical sketches of theses and dissertations in order to protect the identity of NJIT graduates and faculty.

## **ABSTRACT**

### **HIGH PERFORMANCE LATTICE BOLTZMANN METHOD YIELD-STRESS CALCULATIONS BASED ON INTRAVITAL IMAGES OF CLOT FORMATION IN LIVE MICE**

**by  
Vishnu Deep Chandran**

Thrombo-embolic infarction is the major cause of mortality and morbidity in the United States, causing over 1 million strokes, heart attacks and other life-threatening thrombotic events each year in the United States. Conversely, deficiencies in these processes result in severe bleeding risks. The ability to access hydrodynamics stresses at which thrombus structure is likely to embolize can provide insight into the thrombogenesis process. Interestingly, the viscoelastic behavior exhibited by the thrombus resembles that of a Bingham fluid - a material that behaves as a rigid body at low stresses but flows as a viscous fluid when the stress exceeds critical yield stress. Hence, we decided to measure the critical yield stress at which the thrombi yield (and possibly emboli). The fluid-induced stresses are calculated via Lattice-Boltzmann fluid dynamic simulation based on in vivo microscopic images of laser injury-induced thrombi and simulation provided critical yield stress information. To our knowledge, this is the first image-based in-vivo assessment of blood clots viscoelastic nature. Furthermore, the outcome of our work can assist in creating simpler thrombogenesis models that can help improve the understanding of risk factors associated with blood clotting, and ideally help researchers to reduce risks of occlusion and embolism in patients.

**HIGH PERFORMANCE LATTICE BOLTZMANN METHOD YIELD-STRESS  
CALCULATIONS BASED ON INTRAVITAL IMAGES OF CLOT  
FORMATION IN LIVE MICE**

**by  
Vishnu Deep Chandran**

**A Thesis  
Submitted to the Faculty of  
New Jersey Institute of Technology  
in Partial Fulfillment of the Requirements for the Degree of  
Master of Science in Chemical Engineering**

**Otto H. York Department of  
Chemical, Biological and Pharmaceutical Engineering**

**May 2017**

Blank Page

**APPROVAL PAGE**

**HIGH PERFORMANCE LATTICE BOLTZMANN METHOD YIELD-STRESS  
CALCULATIONS BASED ON INTRAVITAL IMAGES OF CLOT  
FORMATION IN LIVE MICE**

**Vishnu Deep Chandran**

---

Dr. Roman S. Voronov, Thesis Advisor  
Assistant Professor of Chemical Engineering, NJIT

Date

---

Dr. Sagnik Basuray, Committee Member  
Assistant Professor of Chemical Engineering, NJIT

Date

---

Dr. Max Roman, Committee Member  
Assistant Research Professor of Biomedical Engineering, NJIT

Date

## **BIOGRAPHICAL SKETCH**

**Author:** Vishnu Deep Chandran

**Degree:** Master of Science

**Date:** May 2017

### **Undergraduate and Graduate Education:**

- Master of Science in Chemical Engineering,  
New Jersey Institute of Technology, Newark, NJ, 2017
- Bachelor of Technology in Chemical Engineering,  
Pondicherry University, Pondicherry, India, 2012

**Major:** Chemical Engineering

If God is defined as the one who creates us, then I believe God exists. I believe God exists in form of my parents who not only created me but also did support me with all my decisions in life in every way possible.

This thesis is dedicated to my parents for their relentless care and unconditional love.

## ACKNOWLEDGMENT

I would like to take this opportunity to thank all the people who have been instrumental in making me who I am today. I am thankful to Professor Roman Voronov for his guidance throughout my graduate study and I thank him for all the details of my work. I would like to acknowledge Professor Lawrence F. Brass, Professor Timothy J. Stalker, Professor Scott L. Diamond, the University of Pennsylvania for providing *in vivo* microscopy images for the research and Texas Advanced Computing Center (TACC # TG-BIO160074) for allowing access to their supercomputers. I would like to thank my committee members Professor Sagnik Basuray and Professor Max Roman for being so approachable and their willingness to serve on the Thesis Committee, my fellow lab members and friends for their help and guidance through my graduate study. Above all, the support and love of my parents.

## TABLE OF CONTENTS

<b>Chapter</b>	<b>Page</b>
1 INTRODUCTION.....	1
1.1 Background.....	1
1.2 Objective.....	3
2 METHODOLOGY .....	4
2.1 Experiment .....	5
2.2 Thrombus Imaging .....	5
2.3 Image Processing and 3D Reconstruction.....	7
2.4 Lattice Boltzmann Method (LBM) .....	9
2.5 Simulation Details.....	11
2.6 Shear Stress Calculation .....	12
2.7 Validation .....	13
3 RESULTS AND DISCUSSION.....	14
3.1 Thrombus Morphology Observation .....	14
3.2 Surface Stress Measurements .....	19
4 CONCLUSION .....	21
REFERENCES .....	22

## LIST OF TABLES

<b>Table</b>	<b>Page</b>
2.1 Simulation Parameters.....	12

## LIST OF FIGURES

Figure	Page
2.1 Schematic of the multidisciplinary investigation approach implemented in this research.....	4
2.2 Left to Right, phase contrast and florescence imaging of blood vessel. Florescence imaging provide the ability to mark regions of blood vessel.....	6
2.3 Left to Right, grayscale thrombus image showing fluorescence corresponding CD41 tracer at induction and after certain time, exported to TIFF format.....	7
2.4 Left to right, the thrombus region and illustration of how parabola are fit on the edges to generate 3-D geometry.....	8
2.5 The 3-D reconstruction results.....	9
2.6 D3Q15 lattice representation .....	11
2.7 The stress distribution across the pipe shows the wall stress value to be around $\sim 31 \text{ dyn/cm}^2$ .....	13
3.1 The anti-CD41 (yellow) and anti-P-selectin (blue) put together give the thrombus regions .....	14
3.2 Clockwise plots show the variation of height, length, aspect ratio and area of the thrombi over time .....	15
3.3 Clockwise plots show the variation of height, length, aspect ratio and area of the thrombi core over time .....	16
3.4 Clockwise plot show thrombus length, height, aspect ratio and area on a nondimensionalizaed scale for 10 different experiments .....	17
3.5 Clockwise plots show thrombus core length, height, aspect ratio and area on a nondimensionalizaed scale for 10 different experiments .....	18
3.6 Tecplot visualization of blood velocity in the vessel and surface stress distribution on for the thrombus at time: 179.51 s.....	20

**LIST OF FIGURES**  
**(Continued)**

<b>Figure</b>	<b>Page</b>
3.7 Global average velocity and surface stress distribution over time for the thrombus .....	19

## LIST OF SYMBOLS

$\nu$	Dynamic Viscosity
$\Omega$	Collision Operator
$\tau$	Relaxation Time
$\sigma$	Shear Stress Tensor

# CHAPTER 1

## INTRODUCTION

### 1.1 Background

Thrombo-embolic infarction is the major cause of mortality and morbidity in the United States. This assembly of platelet deposits and fibrin polymerization gives rise to over one million strokes and other life-threatening thrombotic events each year in the US. Conversely, deficiencies in these processes result in bleeding risks that confront surgeons on a regular basis. Unfortunately, despite tremendous efforts in understanding thrombosis, what causes a thrombus to break apart is less understood. A thrombus deforms before it breaks. For this reason, knowing the extent to which a thrombus can resist deformation, i.e., the measure of stiffness, will provide information on when it is likely to break.

For several decades, researchers have been extensively trying to estimate the viscoelastic properties to understand thrombotic events. For instance, an *in vitro* study estimated the shear elasticity modulus and viscosity of a porcine blood clot using shear-wave dispersion ultrasound vibrometry (Huang et al.). They estimated the shear elasticity modulus and viscosity of a thrombus based on shear-wave propagation speed for an applied acoustic force through the thrombus. Yet another work measured the elasticity modulus using shear-wave ultrasound imaging of a thrombus (Mfoumou et al.). They surgically induced a venous thrombus on jugular vein of a rabbit and monitored the thrombus properties *in vivo*. In the world of biomechanics, stiffness is not a fixed measure. It varies based on the configuration of load and deformation(Baumgart).

*In vivo* a thrombus deforms under the influence of hydrodynamic force acting on it. However, the previous studies did not consider the deformation of a thrombus under this force and the direction at which the ultrasound was passed is not same as the direction of flow. It is to be noted that structural properties of naturally formed material are subjective to internal architecture and composition. For instance, bone has a high compressive strength, but a very low shear stress strength, because of the way it is naturally formed. Similarly, thrombi are heterogeneous material and the hemostatic response produces a hierarchical structure (Stalker et al.). The structural properties of thrombi will be directional in nature. The ability of thrombi to resist deformation will not be the same in all directions. Additionally, assumptions and approximations associated with using parametrize correlation to evaluate viscoelastic properties add a certain degree of error to the estimated properties. Thus, previous approaches of estimating viscoelastic properties of thrombi are not representative of the actual physiology of the process and neither can they provide information on when a thrombus might embolize. To compensate, the viscoelastic properties of a thrombus have to be measured for the deformation along the direction of flow under hydrodynamics conditions.

On the other hand, computer simulations of thrombogenesis are either limited to 2-D or model only some aspects of the process, while omitting others for simplicity (Leiderman and Fogelson; Xu et al.). Thrombogenesis is a combination of the coagulation cascade consisting of a multitude of chemical reactions coupled with cell signaling, fluid dynamics and biomechanics. Therefore, the bottom-up approach taken by the conventional studies rely on calculating discrete platelet dynamics and are based on various assumptions. Hence, a semi-empirical approach might avoid the difficulties

associated with bottom-up modeling. Remarkably, Intravital confocal microscopy is capable of providing information on thrombi structure with a single platelet resolution. To this end, by coupling intravital microscopic time-lapse images with CFD, one can bypass the generation of clot structure dynamics mathematically and avoid the pitfalls associated with bottom-up approach modeling. Thus, a combination of *in vivo* experiments, biomedical imaging and simulation will likely fill the void between the actual physiology of the process and inadequate experimentation.

## 1.2 Objective

Interestingly, the viscoelastic behavior exhibited by the thrombi resembles that of a Bingham fluid - a material that behaves as a rigid body at low stresses but flows as a viscous fluid when the stress exceeds critical yield stress. Hence, we decided to measure the critical yield stress at which the thrombi yield.

The overall aim of the research is to estimate the critical yield stress when thrombi yield under hemodynamic conditions and possibly emboli based on *in vivo* images obtained from experiment on mice using image processing and fluid dynamic simulation.

## CHAPTER 2

### METHODOLOGY

The schematic representation in Figure 2.1 shows the multidisciplinary investigation approach implemented in this research. Some details of the methodology were referred from (Voronov).

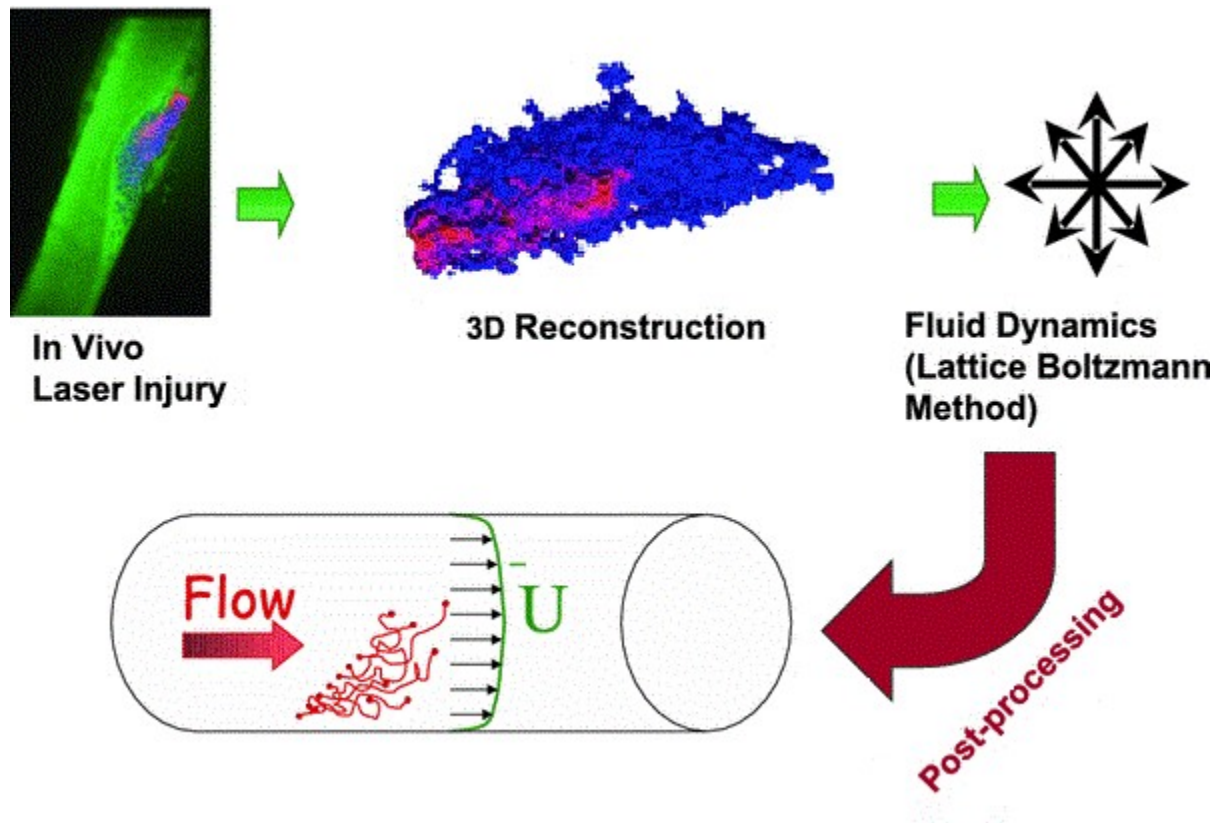


**Figure 2.1** Schematic of the multidisciplinary approach implemented in this research. Source: Voronov, Roman S. et al. "Simulation of Intrathrombus Fluid and Solute Transport Using *in vivo* Clot Structures with Single Platelet Resolution." *Annals of biomedical engineering* 41.6 (2013): 1297–1307.

## **2.1 Experiment**

All experiments were performed at Dr. Lawrence (Skip) Brass's Lab, Perelman School of Medicine, University of Pennsylvania. The experiments were performed in wild-type male mice, on procedures approved by Instructional Animal Care and Use committee (IACUC), University of Pennsylvania. The mice used in the study were of 8-12 weeks of age and a penetrating laser injury induced the thrombi in cremaster muscle microcirculations of the mice. Arterioles (diameter 30-40  $\mu\text{m}$ ) with unperturbed blood flow were selected for the study. A pulsed nitrogen dye laser (440 nm) focused using a microscopic objective induced vascular injury. Antibodies, anti-CD41F(ab)<sub>2</sub>, anti-P-selectin and anti-fibrin were introduced in the blood circulation via the jugular vein. Antibodies were labeled with Alexa-fluor dye monoclonal antibody labeling kits, to aid visualization of thrombi structure. Figure 2.2 shows the difference between phase contrast and fluorescence imaging of blood vessel. Optical Doppler velocimetry to measure the centerline blood velocity in the mice. The velocity measurement was made in a region away from the thrombus such that velocity field was not influenced by its presence and velocimetry measured an average blood vessel velocity of 4.78 mm/s (Stalker et al.).

## **2.2 Thrombi Imaging**

The fluorescently labeled antibodies seek specific proteins expressed by platelets. The CD41 is a membrane proteins that is expressed by fibrinogen receptors of platelets during coagulation. Whereas, P-selectin are adhesion proteins expressed primarily on activated platelets at the sites of vascular injury. When platelets interact with various components

of the sub-endothelial matrix, adhesion and activation of platelets takes place accompanied by the exposure of P-selectin. Thus, when CD41 and P-selectin are expressed the corresponding antibodies anti-CD41F(ab)<sub>2</sub>, anti-P-selectin emit fluorescence after being excited by solid-state lasers.

The cremaster microcirculations of mice were visualized using a spinning disk confocal microscope with a 60X objective. Solid-state lasers (488 nm, 568 nm, 640nm) were used as the fluorescence excitation light source. The region corresponding to CD41 and P-selective expression were imaged. Confocal microscopic images were acquired using CoolSnap HQ CCD digital camera. Slidebook 5 image acquisition and analysis software was used to synchronize and control the microscope, confocal scanner, lasers and camera. events within this over time was determined (Suppl Fig 2A). The thrombi growth were observed for period of 4 minutes. The time-lapse images contained fluorescent channels of intensities, corresponding to fluorescence emitted by tracers marking different regions of the thrombus. The capture were stored in 16-bit grayscale Tagged Image File Format.

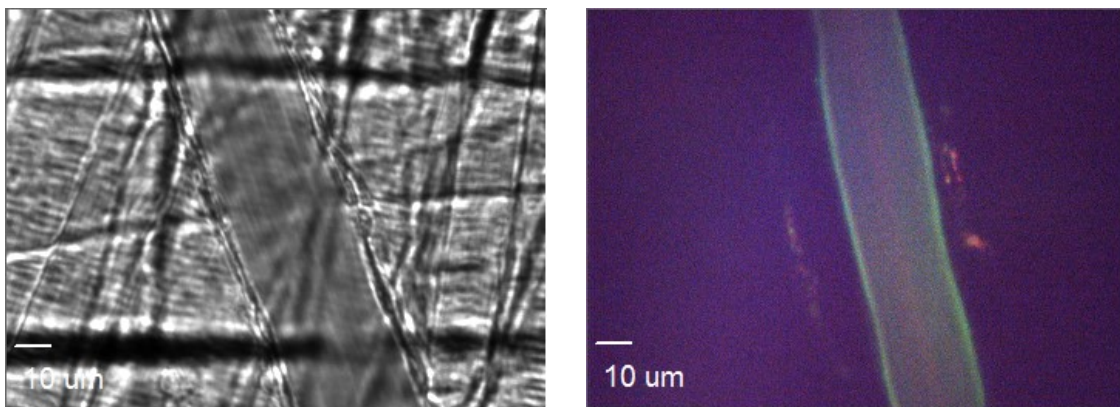


**Figure 2.2** Left to right, phase contrast and fluorescence imaging of blood vessel. Fluorescence imaging provides the ability to mark regions of blood vessel.

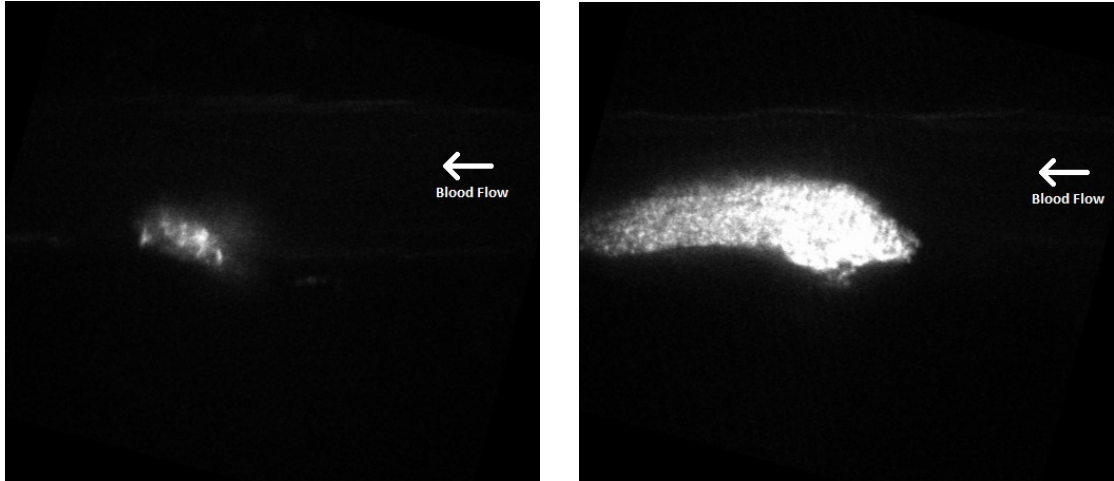


**Figure 2.3** Left to right, grayscale thrombus image showing fluorescence corresponding CD41 tracer at induction and after certain time, exported to TIFF format.

### **2.3 Image Processing and 3-D Reconstruction**

The images of experiment were jittery in nature and were stabilized using Fiji plugins and an in house Matlab®. To achieve primary stabilization, all intensity channels were combined and stabilized using either StackReg or Image Stabilizer ImageJ plugin. The choice of plugin depended on the stabilization achieved. The StackReg plugin essentially align or match stack of image slices by using each slice as the template for the next slice (Thevenaz et al.), where as the Image Stabilizer plugin uses the initial slice in an image stack as the reference and estimates the geometrical transformation needed to best align each of the other slices (Li). Later the stabilization achieved on the combined stacks were applied to the individual all intensity channels. The in house Matlab® code read the translation from the combined image stacks and reapplied to the individual channels based on the custom red-dot algorithm.

Yet another in-house Matlab® code produced 3-D reconstruction of thrombi geometry and the blood vessel from the 2-D images. The code found the best orientation based on the fitting a bounding box on the thrombus (assuming the maximum bounding box length would be obtained when the clot was horizontally aligned) and additional user inputs that mark the blood vessel alignment. The code applies several morphological operations and segmentation techniques to segment the thrombi geometry. Assuming that area of the thrombus would be the largest, the noise from the image were removed. Manually drawn lines on the images masked the blood vessel boundary and helped measurer the blood vessel diameter. To obtain 3-D thrombus geometry from the 2-D measurement, a parabolic curve was fit in the direction perpendicular to blood flow on the thrombus edges by assuming a constant thrombus height to width ratio measured from experiments (Stalker et al.). The thrombus geometry was attached to inner surface of a blood vessel. The blood vessel was constructed as a pipe using the measured blood vessel width as diameter and length three times the diameter of to avoid entrance effect.

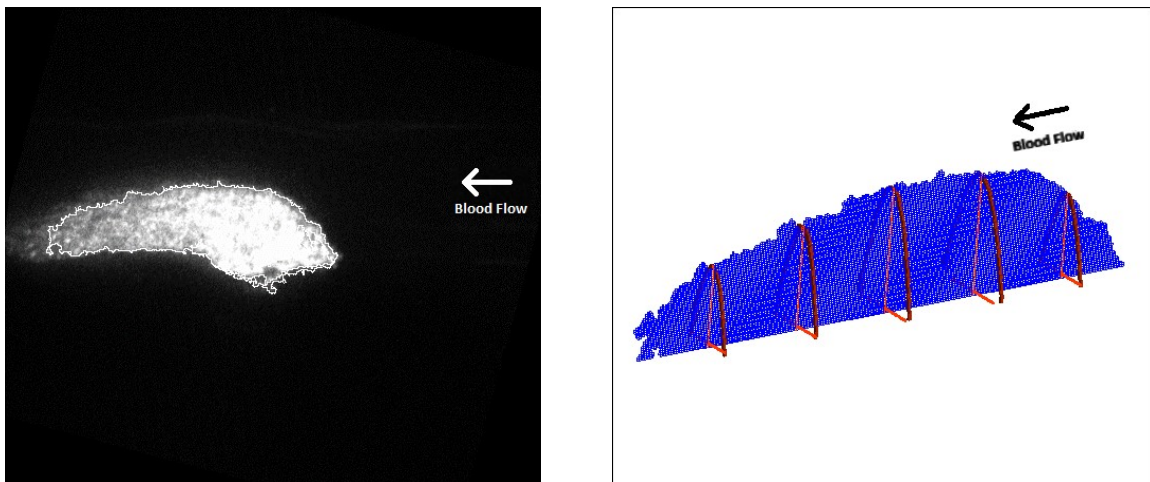


**Figure 2.4** Left to right, the thrombus region and illustration of how parabola are fit on the edges to generate 3-D geometry .



**Figure 2.5** The 3-D reconstruction result.

#### **2.4 Lattice Boltzmann Method (LBM)**

Convective blood flow in the blood vessel was modeled using lattice Boltzmann method (LBM). LBM relies on the discrete Boltzmann equations to simulate fluid flow rather than Navier-Stokes equations as in conventional CFD solvers (Chen and Doolen; Succi; Sukop and Thorne). LBM has computational advantage since it is massively parallelizable on high-end parallel computers (Kandhai et al.; Wang et al.), LBM techniques have been used in a wide spectrum of applications [turbulence (Cosgrove et al.), non-Newtonian flow (Boyd et al.; Gabbanelli et al.; Yoshino et al.), and multiphase flow (Swift et al.). More importantly, for the present application, LBM is especially appropriate for modeling the flow in the microcirculations of mice due its simplicity of reducing the particle velocity space to only a very few discrete points without seriously degrading hydrodynamics and ability to preserve the hydrodynamic moments such as mass density and momentum fluxes, and the necessary symmetries.

The Boltzmann equation is an evolution equation for a particle distribution function, which is calculated as a function of space and time (McNamara and Zanetti) as follows:

$$f(\vec{x} + \vec{e}\Delta t, t + \Delta t) = f(\vec{x}, t) + \Omega(\vec{x}, t) \pm ff \quad (2.1)$$

where,  $x$  is position,  $t$  is time,  $\Delta t$  is the time step,  $e$  is the microscopic velocity,  $\Omega$  is the collision operator,  $f$  is the particle distribution function,  $f^{eq}$  equilibrium particle distribution function and  $ff$  is the forcing factor. The terms on the right hand side of Equation (1) constitute the three steps of the LBM algorithm, namely the streaming, collision and forcing steps. In the streaming step, the particle distribution function  $f$  at position  $x$  and time  $t$  moves in the direction of the velocity to a new position on the lattice at time  $t+\Delta t$ . The collision step subsequently computes the effect of the collisions that have occurred during the movement in the streaming step, which is considered a relaxation towards equilibrium. We use the single-relaxation time approximation of the collision term given by Bhatnagar, Gross and Krook (Bhatnagar et al.).

$$\Omega(\vec{x}, t) = -\frac{1}{\tau}(f - f^{eq}) \quad (2.2)$$

A custom in-house code (Voronov) was used for simulating the convective blood flow. The in-house code used in this work is a Fortran 90 code that was parallelized with Message Passing Interface (MPI). The three-dimensional, 15-velocity lattice (D3Q15) was used to perform the simulations i.e., the particles can stream in 15 different paths (Qian et al.). The lattice nodes included nodes that are in the flow field and nodes that

make up the rigid wall. The fluid particle distribution is simply zero for all wall nodes, avoiding the need to use elaborate meshing techniques near the boundaries.

## 2.5 Simulation Details

A constant pressure drop was imposed across the channel and the pressure drop was estimated based on Hagen–Poiseuille equation using the centerline average blood velocity value obtained *in vivo* by the Doppler velocimetry. The no-slip boundary condition was applied at the wall faces using the bounce-back technique (Sukop and Thorne). Table 2.1 shows the input parameter used for the simulation.

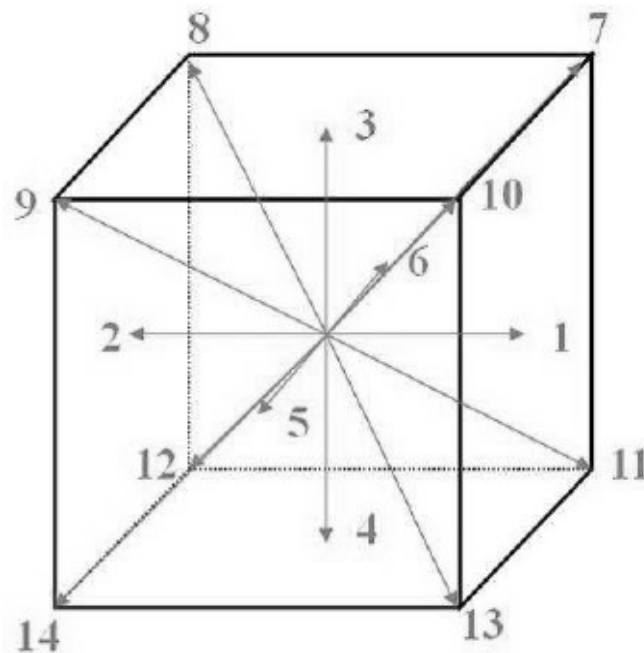


**Figure 2.6** D3Q15 lattice representation.

Source: Wang, Yan, et al. “Three-Dimensional Lattice Boltzmann Flux Solver and Its Applications to Incompressible Isothermal and Thermal Flows.” *Communications in Computational Physics*, 18.3 (2015): 593–620.

**Table 2.1** Simulation Parameters.

<b>Parameter</b>	<b>Value</b>
Kinematic Viscosity	0.03 [cm <sup>2</sup> /s]
Density	0.99 [g/cm <sup>3</sup> ]
Forcing Factor (dP/L)	63034.36 [dyn/cm <sup>3</sup> ]

The simulation was considered converged when the average velocity varied less than 1%. Convergence was monitored every 2000 LBM steps. Approximately 8000 LBM steps were required for full convergence. The average simulation runtime for each geometry for the corresponding time step on Texas Advanced Computing Center (TACC)'s Supercomputer, STAMPEDE, was 3.2 wall clock hours. The simulations were run using 32 MPI processes on 2 nodes (16 cores/node).

## 2.6 Shear Stress Calculation

The shear stress was estimated following the scheme suggested by (Porter et al.). The blood was assumed to be Newtonian fluid and the shear stresses acting on the thrombi surface were estimated as:

$$\sigma = \frac{1}{2} \nu (\nabla \bar{U} + \nabla \bar{U}^T) \quad 2.3$$

where  $\sigma$  is the shear stress tensor,  $\nu$  the dynamic viscosity and  $\nabla \bar{U}$  is derivatives of the the 3-D velocity vector. The derivatives of the velocity field is calculated using a 2nd, order accurate centered difference approximation. The  $3 \times 3$  partials matrix for each point in the field was added to its transpose to produce a symmetric strain matrix. The eigenvalues of the symmetric matrix are found using the Jacobi method and largest absolute-value eigenvalue are used to determine shear stress.

## 2.7 Validation

To validate the model, the upstream wall stress value obtained from stimulation were compared to experimentally obtained value. The average wall shear value from simulation was  $\sim 31 \text{ dyn/cm}^2$ , which is comparable with experimental value of  $40 \text{ dyn/cm}^2$  from literature (Lipowsky et al.).

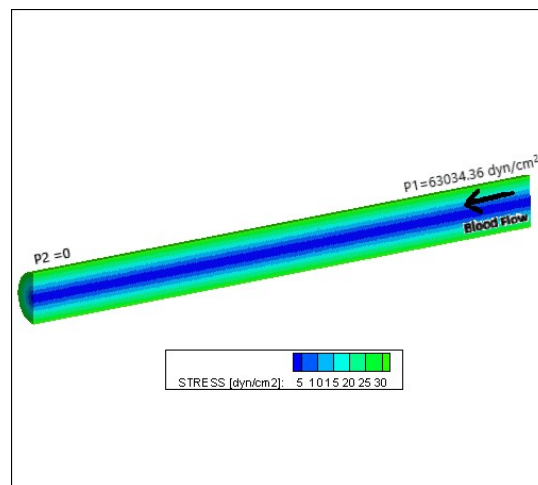


**Figure 2.7** The stress distribution across the pipe shows the wall stress value to be around  $\sim 31 \text{ dyn/cm}^2$ .

## CHAPTER 3

### RESULTS AND DISCUSSION

#### 3.1 Thrombus Morphology Observation

The in-house Matlab® code processed the *in vivo* images and extracted pixel information corresponding to that of the thrombus and its core. The fluorescence intensities measured for both anti-CD41 and anti-P-selectin, essentially give thrombus morphology measurements. The intensities corresponding to that of anti-P-selectin label the thrombus core. Figure 3.1 shows the boundaries marking the core and rest of the thrombus. The post processing of images provided information such as the height, length, aspect ratio, and area of the thrombus and its core for every time step. The measurements were converted to scale by multiplying the values with the resolution at which they were captured (i.e., 0.267 microns per pixel). Figure 3.2 shows the typical evolution details of the thrombus and its core over time.

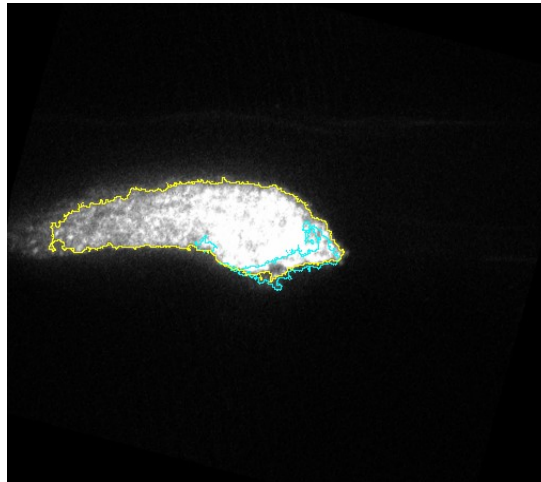


**Figure 3.1** The anti-CD41 (yellow) and anti-P-selectin (blue) put together give the thrombus.

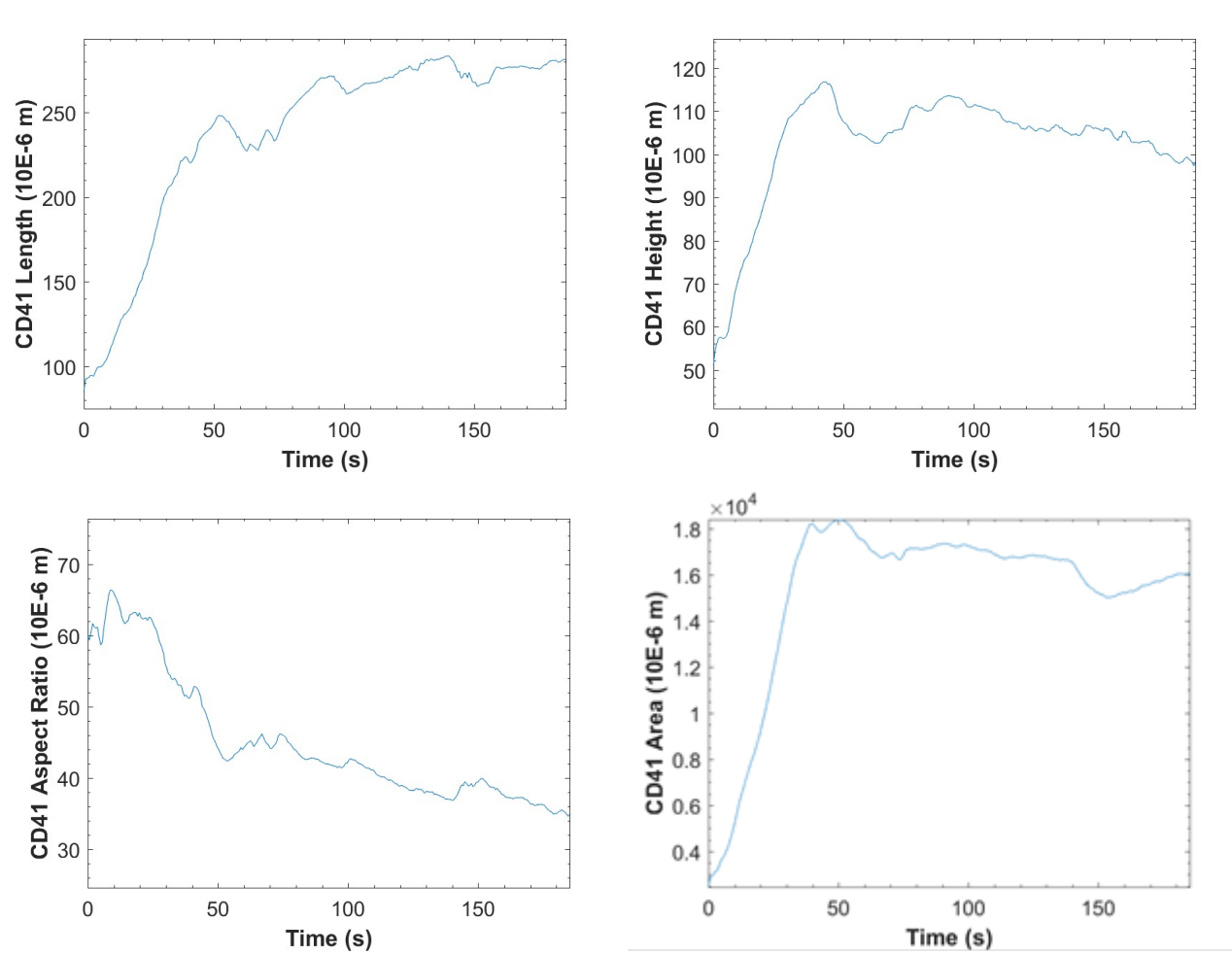


**Figure 3.2** Clockwise plots show the variation of height, length, aspect ratio and area of the thrombi over time.

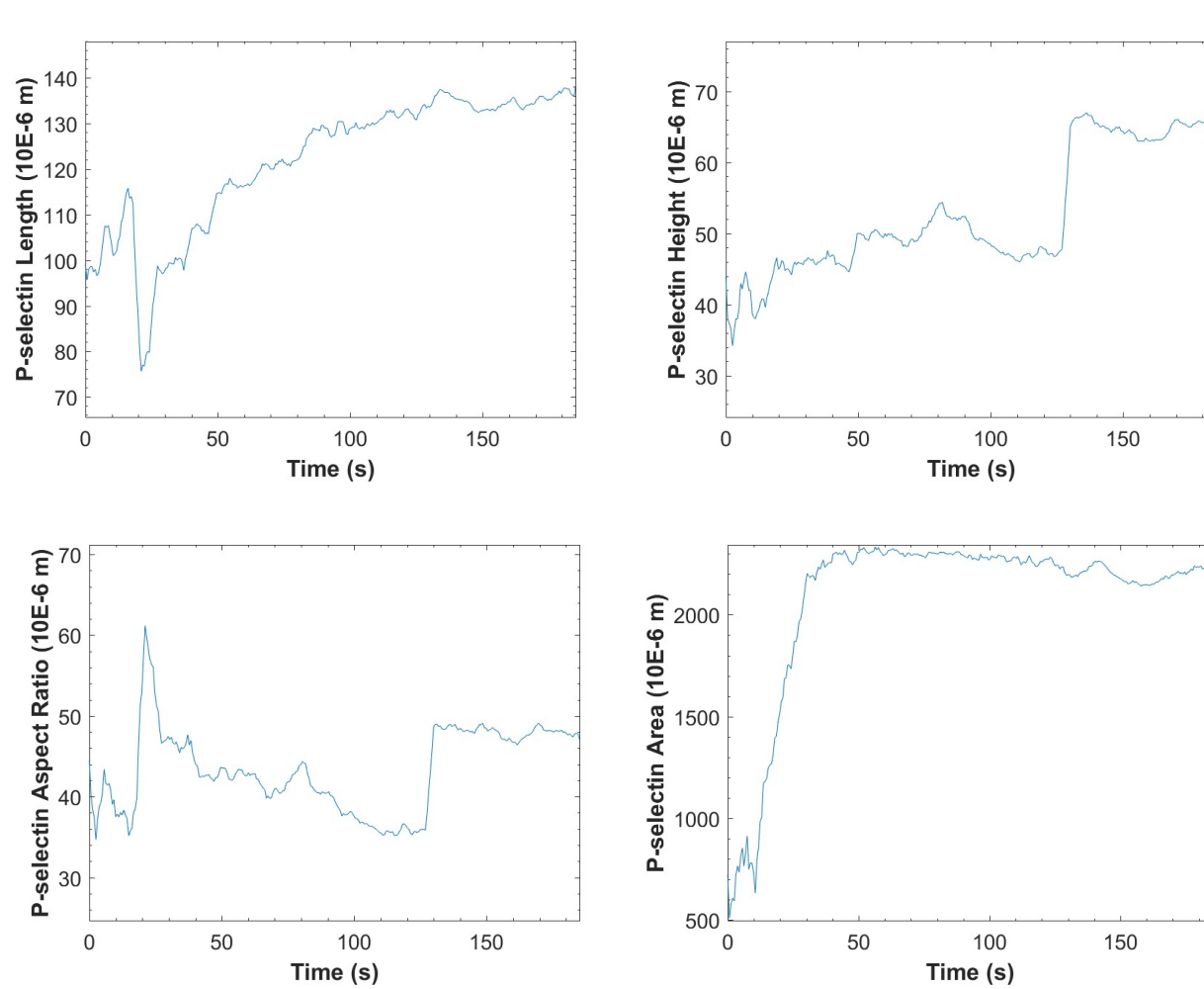


**Figure 3.3** Clockwise plots show the variation of height, length, aspect ratio and area of the thrombi core over time.

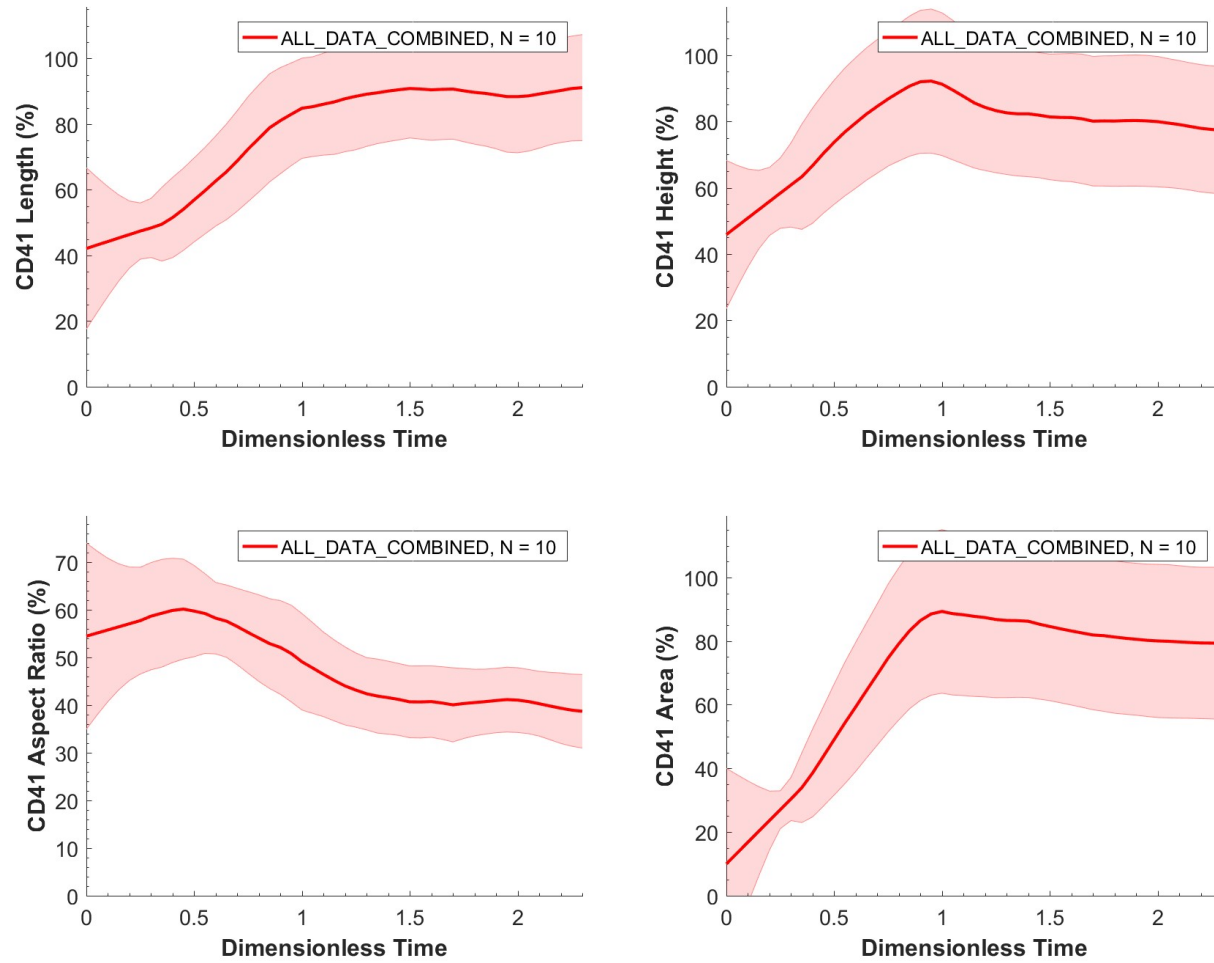


**Figure 3.4** Clockwise plot show thrombus length, height, aspect ratio and area on a nondimensionalized scale for 10 different experiments.

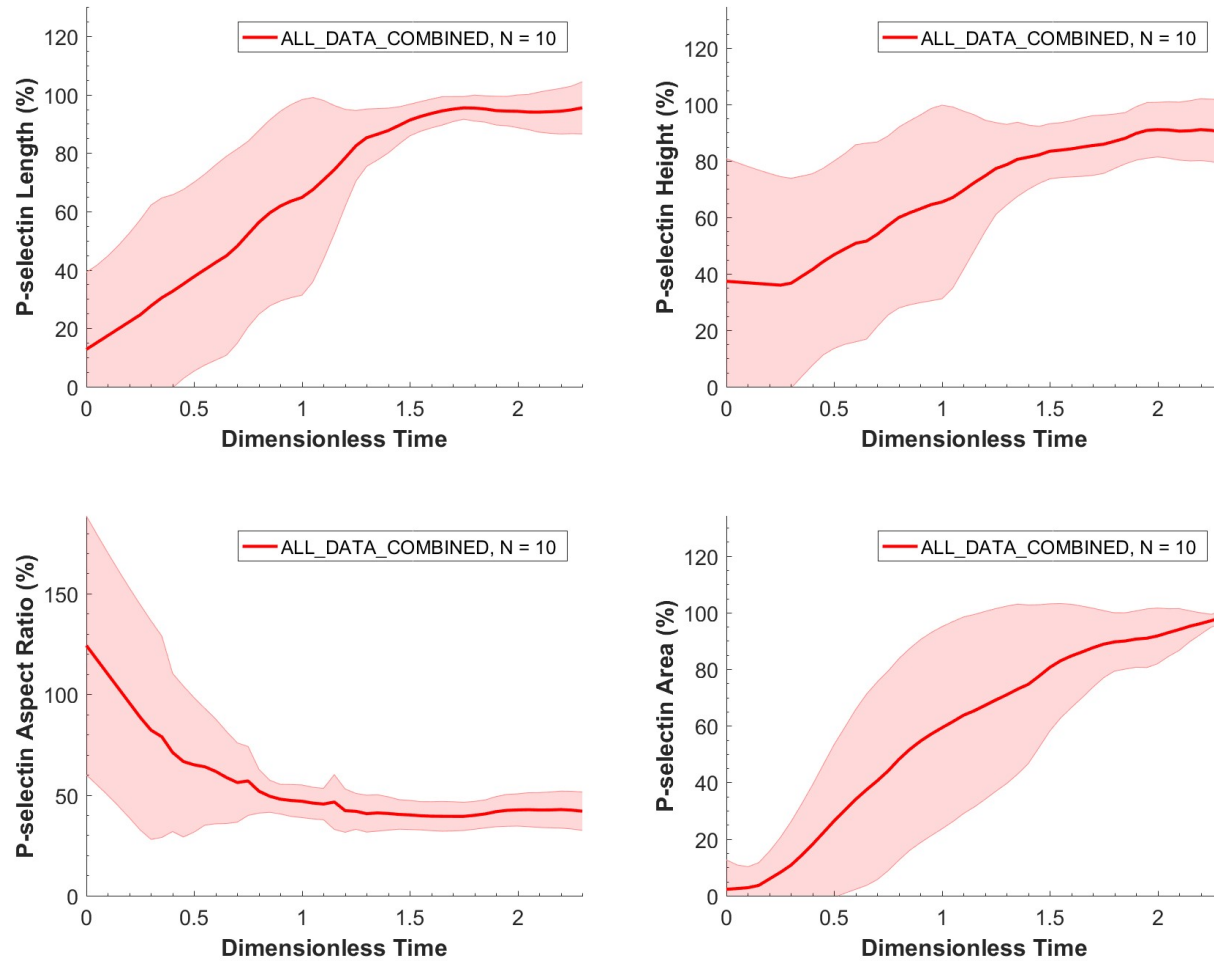


**Figure 3.5** Clockwise plots show thrombus core length, height, aspect ratio and area on a nondimensionalized scale for 10 different experiments.

In order to compare all clots on the same time scale, we nondimensionalized the data. Nondimensional time was obtained by dividing the absolute time scale by the critical time at which thrombus attains maximum area. Once nondimensionalized, the resulting data collapses onto a single curve as illustrated in Figure 3.4 and Figure 3.5 shown a function of the nondimensionalized time,  $t^*$ . It is observed that, although each clot seems different from the other, all thrombogenesis behavior looks the same when compared on a nondimensional scale.

Despite the underlying complexity, it has been observed that the thrombogenesis mechanism consists of several discrete regimes common to all blood clots (shown in Figure 3.4 and 3.5). That is, after initial attachment, the thrombi experience uniform growth followed by a critical event that marks a transition from transient morphology to steady state stability. This sheds hope that a uniform theory of thrombogenesis can be developed that will describe all clotting events using a single analytical equation. During the critical event, platelet mass from the upstream portion of the thrombus yields to the surrounding blood flow and rearranges to minimize drag on the clot

### **3.2 Surface Stress Measurements**

Figure 3.6 shows a Tecplot visualization of velocity and surface stress distribution. The velocity and surface stress values were obtained from Lattice Boltzmann simulation at a constant pressure drop. The surface stress values varied from a minimum of  $\sim 6.31 \times 10$  dyn/cm<sup>2</sup> to a maximum of  $\sim 442.24$  dyn/cm<sup>2</sup>. Figure 3.7 shows the global average velocity and surface stress distribution over time for the thrombus.

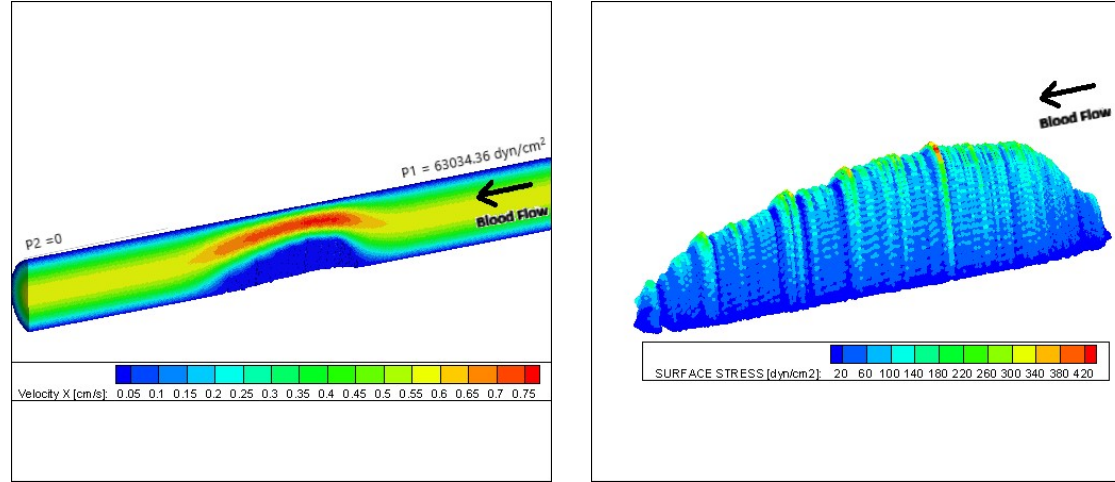


**Figure 3.6** Tecplot visualization of blood velocity in the vessel and surface stress distribution on for the thrombus at time: 179.51 s.

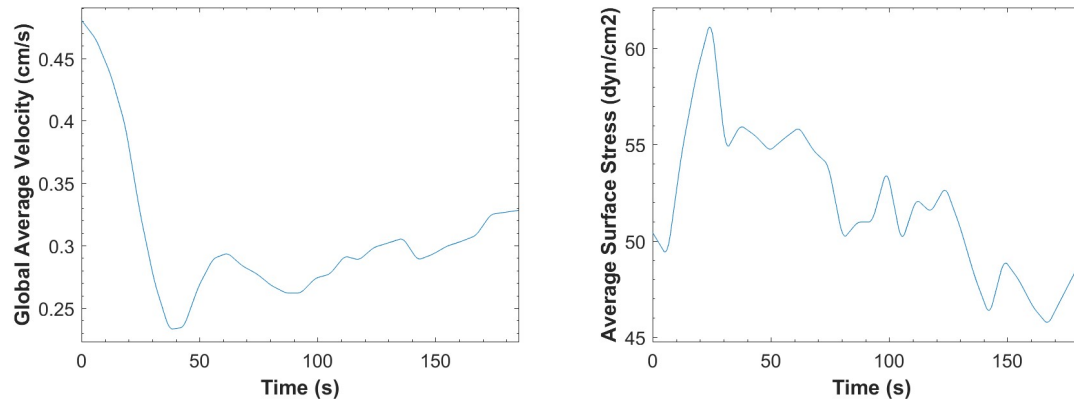


**Figure 3.7** Global average velocity and surface stress distribution over time for the thrombus.

## **CHAPTER 4**

### **CONCLUSION**

To our knowledge, this is the first image-based in-vivo assessment of blood clots viscoelastic nature. Collectively, the outcome of this work is expected to provide insight towards an understanding of clot generation, its structure, stability, thromboembolism and coagulopathy. Moreover, they can assist in creating simpler thrombogenesis models that can help improve the understanding of risk factors associated with blood clotting, and ideally help researchers to reduce risks of occlusion and embolism in patients.

## REFERENCES

- Baumgart, F. "Stiffness - an Unknown World of Mechanical Science?" *Injury*, vol. 31, no. 2, 2000, pp. 14-23.
- Bhatnagar, Prabhu Lal et al. "A Model for Collision Processes in Gases. I. Small Amplitude Processes in Charged and Neutral One-Component Systems." *Physical review*, vol. 94, no. 3, 1954, p. 511.
- Boyd, J. et al. "A Second-Order Accurate Lattice Boltzmann Non-Newtonian Flow Model." *Journal of Physics A: Mathematical and General*, vol. 39, no. 46, 2006, p. 14241.
- Chen, Shiyi and Gary D. Doolen. "Lattice Boltzmann Method for Fluid Flows." *Annual Review of Fluid Mechanics*, vol. 30, no. 1, 1998, pp. 329-364.
- Cosgrove, J. A. et al. "Application of the Lattice Boltzmann Method to Transition in Oscillatory Channel Flow." *Journal of Physics A: Mathematical and General*, vol. 36, no. 10, 2003, p. 2609.
- Gabbanelli, Susana et al. "Lattice Boltzmann Method for Non-Newtonian (Power-Law) Fluids." *Physical Review E*, vol. 72, no. 4, 2005, p. 046312.
- Huang, Chih-Chung et al. "Estimating the Viscoelastic Modulus of a Thrombus Using an Ultrasonic Shear-Wave Approach." *Medical Physics*, vol. 40, no. 4, 2013, pp. 042901.
- Kandhai, D. et al. "Lattice-Boltzmann Hydrodynamics on Parallel Systems." *Computer Physics Communications*, vol. 111, no. 1, 1998, pp. 14-26.
- Leiderman, Karin and Aaron L Fogelson. "Grow with the Flow: A Spatial–Temporal Model of Platelet Deposition and Blood Coagulation under Flow." *Mathematical Medicine and Biology*, vol. 28, no. 1, 2011, pp. 47-84.
- Li, Kang. "The Image Stabilizer Plugin for Imagej." 2008.  
[http://www.cs.cmu.edu/~kangli/code/Image\\_Stabilizer.html](http://www.cs.cmu.edu/~kangli/code/Image_Stabilizer.html)[http://www.cs.cmu.edu/~kangli/code/Image\\_Stabilizer.html](http://www.cs.cmu.edu/~kangli/code/Image_Stabilizer.html).
- Lipowsky, Herbert H et al. "The Distribution of Blood Rheological Parameters in the Microvasculature of Cat Mesentery." *Circulation research*, vol. 43, no. 5, 1978, pp. 738-749.
- McNamara, Guy R and Gianluigi Zanetti. "Use of the Boltzmann Equation to Simulate Lattice-Gas Automata." *Physical review letters*, vol. 61, no. 20, 1988, p. 2332.

- Mfoumou, Etienne et al. "Time-Dependent Hardening of Blood Clots Quantitatively Measured in Vivo with Shear-Wave Ultrasound Imaging in a Rabbit Model of Venous Thrombosis." *Thrombosis Research*, vol. 133, no. 2, 2014, pp. 265-271.
- Porter, Blaise et al. "3-D Computational Modeling of Media Flow through Scaffolds in a Perfusion Bioreactor." *Journal of Biomechanics*, vol. 38, no. 3, 2005, pp. 543-549.
- Qian, YH et al. "Lattice Bgk Models for Navier-Stokes Equation." *EPL (Europhysics Letters)*, vol. 17, no. 6, 1992, p. 479.
- Stalker, Timothy J. et al. "Hierarchical Organization in the Hemostatic Response and Its Relationship to the Platelet-Signaling Network." *Blood*, vol. 121, no. 10, 2013, p. 1875.
- Succi, S. *The Lattice Boltzmann Equation for Fluid Dynamics and Beyond*. Clarendon Press ; Oxford University Press, 2001.
- Sukop, Michael C. and Daniel T. Jr Thorne. *Lattice Boltzmann Modeling: An Introduction for Geoscientists and Engineers*. Springer Publishing Company, Incorporated, 2006.
- Swift, Michael R et al. "Lattice Boltzmann Simulations of Liquid-Gas and Binary Fluid Systems." *Physical Review E*, vol. 54, no. 5, 1996, p. 5041.
- Thevenaz, Philippe et al. "A Pyramid Approach to Subpixel Registration Based on Intensity." *IEEE transactions on image processing*, vol. 7, no. 1, 1998, pp. 27-41.
- Voronov, Roman. "Fluid Shear Stress and Nutrient Transport Effects Via Lattice Boltzmann and Lagrangian Scalar Tracking Simulations of Cell Culture Media Perfusion through Artificial Bone Tissue Engineering Constructs Imaged with Microct." *School of Chemical, Biological and Materials Engineering*, Doctor of Philosophy, Dissertation, University of Oklahoma, 2010, Advisor, Dimitrios V. Papavassiliou, Vassilios I. Sikavitsas.
- Wang, Junye et al. "Domain-Decomposition Method for Parallel Lattice Boltzmann Simulation of Incompressible Flow in Porous Media." *Physical Review E*, vol. 72, no. 1, 2005, p. 016706.
- Xu, Zhiliang et al. "A Multiscale Model of Venous Thrombus Formation with Surface-Mediated Control of Blood Coagulation Cascade." *Biophysical journal*, vol. 98, no. 9, 2010, pp. 1723-1732.
- Yoshino, M. et al. "A Numerical Method for Incompressible Non-Newtonian Fluid Flows Based on the Lattice Boltzmann Method." *Journal of Non-Newtonian Fluid Mechanics*, vol. 147, no. 1-2, 2007, pp. 69-78.